

Elsevier required licence: © 2021

This manuscript version is made available under the  
CC-BY-NC-ND 4.0 license

<http://creativecommons.org/licenses/by-nc-nd/4.0/>

The definitive publisher version is available online at

<https://doi.org/10.1016/j.watres.2020.116645>

1 **Mechanistic insights into the effect of poly ferric sulfate on anaerobic**  
2 **digestion of waste activated sludge**

3 Xuran Liu<sup>a,b</sup>, Yanxin Wu<sup>a,b</sup>, Qiuxiang Xu<sup>a,b</sup>, Mingting Du<sup>a,b</sup>, Dongbo Wang<sup>a,b\*</sup>, Qi Yang<sup>a,b</sup>, Guojing Yang<sup>c</sup>,  
4 Hong Chen<sup>d</sup>, Tianjing Zeng<sup>e</sup>, Yiwen Liu<sup>f</sup>, Qilin Wang<sup>f</sup>, Bing-jie Ni<sup>f</sup>

5 <sup>a</sup>College of Environmental Science and Engineering, Hunan University, Changsha 410082, P.R. China

6 <sup>b</sup>Key Laboratory of Environmental Biology and Pollution Control (Hunan University), Ministry of Education,  
7 Changsha 410082, P.R. China

8 <sup>c</sup>College of Biological and Environmental Sciences, Zhejiang Wanli University, Ningbo 315100, PR China

9 <sup>d</sup>Key Laboratory of Water-Sediment Sciences and Water Disaster Prevention of Hunan Province, School of  
10 Hydraulic Engineering, Changsha University of Science & Technology, Changsha 410004, China

11 <sup>e</sup>Ecology and Environment Department of Hunan Province, Changsha 410014, P.R. China

12 <sup>f</sup>Centre for Technology in Water and Wastewater, School of Civil and Environmental Engineering, University  
13 of Technology Sydney, Sydney, NSW 2007, Australia

14

15

16 First author: Xuran Liu; E-mail: liuxuran@hnu.edu.cn.

17 Corresponding author: Dongbo Wang; E-mail: w.dongbo@yahoo.com.

18 Tel: +86 731 88823967; fax: +86 731 88822829.

---

## 19 Abstract

20 Poly ferric sulfate (PFS), one of the typical inorganic flocculants widely used in wastewater management  
21 and waste activated sludge (WAS) dewatering, could be accumulated in WAS and inevitably entered in  
22 anaerobic digestion system at high levels. However, knowledge about its impact on methane production is  
23 virtually absent. This study therefore aims to fill this gap and provide insights into the mechanisms involved  
24 through both batch and long-term tests using either real WAS or synthetic wastewaters as the digestion  
25 substrates. Experimental results showed that the maximum methane potential and production rate of WAS  
26 was respectively retarded by 39.0% and 66.4%, whereas the lag phase was extended by 237.0% at PFS of 40 g  
27 per kg of total solids. Mechanism explorations exhibited that PFS induced the physical enmeshment and  
28 disrupted the enzyme activity involved in anaerobic digestion, resulting in an inhibitory state of the bioprocess  
29 of hydrolysis, acidogenesis, and methanogenesis. Furthermore, PFS's inhibition to hydrogenotrophic  
30 methanogenesis was much severer than that to acetotrophic methanogenesis, which could be supported by the  
31 elevated abundances of *Methanosaeta* sp and the dropped abundances of *Methanobacterium* sp in PFS-present  
32 digester, and probably due to the severe mass transfer resistance of hydrogen between the syntrophic bacteria  
33 and methanogens, as well as the higher hydrogen appetency of PFS-induced sulfate reducing bacteria.  
34 Among the derivatives of PFS, "multinucleate and multichain-hydroxyl polymers" and sulfate were unveiled  
35 to be the major contributors to the decreased methane potential, while the "multinucleate and  
36 multichain-hydroxyl polymers" were identified to be the chief buster to the slowed methane-producing rate  
37 and the extended lag time.

38 **Keywords:** Poly ferric sulfate; Waste activated sludge; Anaerobic digestion; Methane production; Hydroxyl  
39 polymers

## 40 **1. Introduction**

41 Poly ferric sulfate (PFS), the polymerized iron salts, can provide a variety of nucleic hydroxyl  
42 high-valence complex ions and hydrolyze to the highly cross-linked hydrophobic multinucleate and  
43 multichain-hydroxyl polymers after dissolving in aqueous phase, making it possess the high coagulation  
44 efficiency (Jiang et al., 1998; Zouboulis et al., 2008). Compared with the conventionally inorganic  
45 coagulants such as ferric chloride and aluminum sulfate, the PFS owns some advantages, such as  
46 comparatively lower dose, wider range of pH and temperature but more effective coagulation properties, and  
47 contains no harmful substances (Jiang et al., 1998).

48 In sewage treatment system, the potential pathway of PFS entering in sewage sludge is the wastewater  
49 pretreatment process, such as the enhanced coagulation and chemical phosphorus removal process (Fig. S1).  
50 In these processes, PFS would firstly hydrolyze to macromolecular iron-polymer containing hydroxyl and  
51 sulfate groups, and then complex and precipitate with phosphorus or sludge flocs, in which most of the PFS is  
52 inevitably absorbed and concentrated in primary sedimentation sludge (PS) (Chu et al., 2018; Moussas et al.,  
53 2009). It was reported that the dosage of PFS in wastewater pretreatment process was generally at 10-60  
54 mg/L and highly depended on the source of wastewater quality (Chu et al., 2018; Zouboulis et al., 2008), with  
55 the potential content of Fe remained in chemically enhanced primary sedimentation sludge being in the range  
56 of 0 to 22 g per kg of total solid sludge (Ghyoot et al., 1997; Lin et al., 2017; Zhou et al., 2020). Moreover,  
57 in some small-scale wastewater treatment plants (WWTPs) where anaerobic digestion of waste activated  
58 sludge (WAS) in-situ in WWTPs is not economically feasible and in some developing countries like China  
59 where most of the WWTPs have not already been configured with anaerobic digesters, WAS is firstly required  
60 to be dewatered and then gathered together for further treatment (Fig. S1). As PFS is substantially added  
61 into WAS during mechanically dewatering process, PFS levels in such sludges are inevitably at high levels.

62 It was reported that PFS content in dewatered sludge was in the range of 10-40 g/kg dry sludge when the PFS  
63 was applied in sludge conditioning (Bratby et al 2016; Watanabe et al., 1999; Wei et al., 2018a). In addition,  
64 according to our survey on 4 WWTPs in Central China, 90% of the PFS used in mechanical dewatering was  
65 remained in dewatered sludge, and the PFS levels in such sludge reached at 3.0-48.5 g/kg TS. Till now,  
66 however, most of the studies on PFS focused on its performance optimization, few considered its  
67 accumulation in sewage sludge (include PS and WAS) and potential impacts on subsequent treatments, such  
68 as anaerobic digestion (Fig. S1).

69 Anaerobic digestion is not only a conventional technology for stabilizing sewage sludge, but also a  
70 developing technology to be regained in energy self-sufficient operation (Appels et al., 2008). Through  
71 anaerobic digestion, the sludge volume can be effectively reduced, the pathogenic microorganisms can be  
72 effectively killed, and more importantly, the carbon substrates can be transferred to renewable energy,  
73 methane (Appels et al., 2008; Zhang et al., 2020). It is known that sludge anaerobic digestion includes  
74 several biological conversions (e.g., hydrolysis, acidogenesis, and methanogenesis) executed by a series of  
75 microbes such as hydrolytic microorganisms, acid-producing microorganisms, and methanogens (Wu et al.,  
76 2020; Zhen et al., 2017). Thus, the accumulated PFS in sewage sludge might affect these bio-conversions,  
77 thereby affecting the performances of sludge anaerobic digestion.

78 When PFS is dissolved in hydrous media such as sewage sludge, sulfate, iron, and their “hydroxyl  
79 polymers” will co-exist. As a compound being rich in iron, PFS would provide the required iron element for  
80 the synthesis of iron-containing enzymes involved in hydrogenotrophic methanogenesis or acetoclastic  
81 methanogenesis, and meanwhile served as a scavenger for  $S^{2-}$  in sludge, which might be beneficial for  
82 methane production (Wei et al., 2018b). As a substance containing sulfate, however, PFS might serve as a  
83 special form of anaerobic respiration and terminal electron-accepting process, and thereby induced the

84 enrichment of sulfate-reducing bacteria (SRB) and competition and/or coexistence with methanogens for  
85 carbon and electrons, as well as the production of hydrogen sulfide, which could result in a shift in the  
86 metabolic pathways of organic substrates and the change of microbial community structure in anaerobic  
87 digestion (Cetecioglu et al., 2019; Hansen et al., 1999; Ozuolmez et al., 2015; Qiao et al., 2016). And as the  
88 “hydroxyl polymers” such as  $\text{Fe}_3(\text{OH})_4^{5+}$ ,  $\text{Fe}_5\text{O}_2(\text{OH})_6^{5+}$ , which play a core role in coagulation process and  
89 have a similar but better performance with ferric hydroxide, may induce the aggregation of sludge flocs and  
90 the alteration of subsequent anaerobic digestion performance (Moussas et al., 2009). The effect of coagulant  
91 (e.g.,  $\text{FeCl}_3$  and PACl) on acidogenic fermentation of PS have been clearly reported by Lin et al. (2017, 2018),  
92 which demonstrated that  $\text{FeCl}_3$  dosed at 10-30 mg Fe/L sewage had little influence on sludge hydrolysis and  
93 volatile fatty acid production, whereas an obvious inhibitory effect was observed for PACl in organic  
94 hydrolysis of the PS. These excellent attempts open the box of coagulant’s effect on anaerobic fermentation  
95 of PS, however, the WAS has different properties compared to PS. For instance, WAS is the sludge produced  
96 by biological process and it mainly contains biomass and extracellular polymeric substances, whereas PS is  
97 the sludge composed of settleable particulate organics removed from wastewater pretreatment processes. Up  
98 to now, however, there is no information available on the effects of PFS, the mixture or synthesis being made  
99 up of sulfate, iron and “hydroxyl polymer”, on the anaerobic digestion of real WAS. And moreover, the  
100 underlying mechanisms and microbial community response to PFS during anaerobic WAS digestion have not  
101 been yet thoroughly investigated.

102 Thus, the main objective of this work is to reveal the effects of PFS on the anaerobic WAS digestion.  
103 Firstly, the effects of PFS at different dosages (0, 5, 10, 20, or 40 g/kg TS) on methane production during  
104 anaerobic WAS digestion was investigated. Then, the underlying mechanisms for PFS affecting the  
105 digestion were identified by assessing its effect on the solubilization of WAS, the processes of WAS

106 hydrolysis, acidogenesis and methanogenesis, the contributions of the intermediates decomposed from PFS to  
107 methane production, the microbial community as well. To our knowledge, this is the first work reporting the  
108 adverse effects of PFS on the anaerobic digestion of real WAS. The findings obtained will provide insights  
109 into the PFS-involved anaerobic digestion system and are supposed to make a sound contribution to mitigate  
110 PFS's negative effects in the future.

## 111 **2. Materials and methods**

### 112 **2.1. WAS and PFS**

113 The WAS used in this study was obtained from the secondary sedimentation tank of a WWTP with  
114 sludge retention time of 20 d in Changsha, China, where PFS was not used in wastewater treatment. The  
115 WAS was concentrated by gravity thickening at 4 °C for 24 h and screened with a 1 mm sieve to remove  
116 impurities before use. The main characteristics of used WAS were as follows: pH  $6.8 \pm 0.1$ , total solids (TS)  
117  $38300 \pm 600$  mg/L, volatile solids (VS)  $24800 \pm 350$  mg/L, soluble chemical oxygen demand (COD)  $170 \pm 10$   
118 mg/L, total COD  $37000 \pm 420$  mg/L, total carbohydrate  $3900 \pm 160$  mg COD/L, and total protein  $17800 \pm 220$   
119 mg COD/L. The seed sludge was collected from an anaerobic digester fed with WAS in our lab, and its main  
120 characteristics were: pH  $6.9 \pm 0.1$ , TS  $16500 \pm 320$  mg/L, VS  $12300 \pm 350$  mg/L, total COD  $19800 \pm 380$   
121 mg/L, specific activity on acetate  $0.12$  g CH<sub>4</sub>-COD/g (VS·d). The PFS used in this study was purchased  
122 from Chongqing Reagent Company, which has a total iron value of 20%, and with a residual ferrous content  
123 less than 0.1%.

### 124 **2.2. Methane production during WAS anaerobic digestion in the presence of different PFS** 125 **levels**

126 Anaerobic digestion of WAS in the presence of different PFS levels was conducted through batch  
127 experiments in five replicate serum reactors each with a working volume of 1.0 L. First, each reactor was

128 fed with 800 mL WAS. Afterward, different volumes of PFS solution (3% w/w) were added into those  
129 reactors to achieve the predetermined dosage at the beginning of the experiment, followed by 120 rpm of  
130 stirring for 2 min and 60 rpm for 10 min (Zhang et al., 2018; Zouboulis et al., 2008). The predetermined  
131 dosages of PFS addition were 0 (control), 5, 10, 20, and 40 g/kg TS, respectively. Next, 400 mL of seed  
132 sludge was equally divided and added before the pH of these five reactors was adjusted to  $7.0 \pm 0.1$  with 4 M  
133 hydrochloric acid or 4 M sodium hydroxide. Then, each reactor was diluted with Milli-Q water to 1.0 L.  
134 To exclude the methane production from seed sludge, one blank reactor contained 80 mL of seed sludge and  
135 920 mL of Milli-Q water was also operated. Oxygen in all the reactors was removed by purging with  
136 nitrogen gas for 5 min. After that, all reactors were capped with rubber stoppers, sealed, and incubated at  $35$   
137  $\pm 1$  °C in an air-bath shaker (120 rpm). The pH of all reactors was controlled at  $7.0 \pm 0.1$  in the whole  
138 digestion period. The biogas yield, methane and H<sub>2</sub>S content in biogas were determined every 2 days. The  
139 calculation of the cumulative volume of methane was detailed in our previous publications (Wang et al., 2018).  
140 It should be noted that all tests were conducted in triplicate in this study, and the methane production reported  
141 were net values with the values measured in blank excluded.

### 142 **2.3. Effect of PFS on solubilization, hydrolysis, acidogenesis, and methanogenesis of anaerobic** 143 **digestion**

144 In the digesters operated above, the concentration of soluble protein (carbohydrate) in digestion  
145 supernate, VSS reduction and floc size of sludge were analyzed after digestion of 3 days, and by comparing  
146 these results, the impact of PFS on solubilization process could be indicated. To assess the effect of PFS on  
147 the processes of hydrolysis, acidogenesis, and methanogenesis, the following batch tests using synthetic  
148 wastewaters were carried out (Angelidaki et al., 2009; Wang et al., 2018). Twelve reactors with working  
149 volume of 1.0 L each were first divided into four groups (Test-I, Test-II, Test-III, and Test-IV) with three in

150 each. Test-I, Test-II, Test-III, and Test-IV were respectively used to evaluate the impact of PFS on hydrolysis,  
151 acidogenesis, acetotrophic methanogenesis, and hydrogenotrophic methanogenesis. All these tests were  
152 lasted for 3 d.

153 Test-I: The three reactors received 920 mL synthetic wastewater and 80 mL of the same seed sludge  
154 collected from a laboratory anaerobic sludge digester. The synthetic wastewater contains 6.0 g BSA and 1.2  
155 g dextran. Two reactors were respectively fed with 0.15 and 0.60 g PFS (the amount of PFS is equal to that  
156 in the 5 and 20 g/kg TS PFS digester, respectively) while the other reactor received no PFS and was set as the  
157 control. All other conditions were the same as those described above. By measuring the degradation rates  
158 of protein and dextran, the effect of PFS on hydrolysis process could be indicated.

159 Test-II: This test was operated the same as that described in Test-I except that the substrates (i.e., BSA  
160 and dextran) in synthetic wastewater were replaced by 4.0 g L-alanine (model amino acid compound) and 0.8  
161 g glucose (model monosaccharide compound), respectively.

162 Test-III: The operation of this test was performed with the same approach as that described in Test-I  
163 except that 3.0 g sodium acetate was employed to replace BSA and dextran in synthetic wastewater.

164 Test-IV: The operation of this test was performed with the same approach as that described in Test-I  
165 except that the mixture of standard gas (40% hydrogen, 10% carbon dioxide and 50% nitrogen) was employed  
166 to replace BSA and dextran in gas and liquid phase by flushing the configured standard gas for 5 min.

#### 167 **2.4. Identifying the effect of components of PFS on methane production**

168 As mentioned above, the chemical components of PFS can be divided into three types: hydroxyl  
169 polymers, iron, sulfate in hydrous media and sediments. The addition of PFS would introduce these three  
170 components into the digestion system, which might have different effects on anaerobic digestion. To reveal  
171 this question, the following batch test was carried out using real sludge as the digestion substrates. In this

172 test, 5 replicate serum bottles with identical working volume (1.0 L) were performed, and each received 800  
173 mL WAS. Among them, one was served as the control without addition of any chemical, while the other 4  
174 bottles received 20 g/kg TS PFS, 11.6 g/kg TS ferric chloride, 20.6 g/kg TS potassium sulfate, or 14.3 g/kg TS  
175 ferric sulfate, respectively. It should be noted that ferric chloride and potassium sulfate were set as substitute  
176 for iron and sulfate to evaluate their effect on methane production, respectively, with their initial  
177 concentrations selected based on the stoichiometric content of iron and sulfate in 20 g/kg TS PFS. Because  
178 the hydroxyl polymers cannot be modeled, the ferric sulfate was used as a substitute for co-exist of iron and  
179 sulfate to qualitatively reflect its effect on methane production.

180 After the addition of the chemicals, all the bottles were diluted with Milli-Q water to 920 mL and  
181 inoculated with 80 mL seed sludge. After flushing with nitrogen gas for 5 min to remove oxygen, all bottles  
182 were sealed closely and placed in an air-bath shaker (120 rpm) under  $35 \pm 1$  °C. All other operating steps  
183 were the same as those mentioned in Section 2.2.

## 184 **2.5. Long-Term operation of semi-continuous digesters for microbial activities and community** 185 **measurement**

186 To reveal the effect of PFS on anaerobic digestion of WAS from the point of microbial activities and  
187 community, two semi-continuous digesters were operated in this work. The two reactors were fed with  
188 either 0 or 20 g/kg TS PFS-added sludge, with the 20 g/kg TS chosen as the representative dosage of PFS in  
189 the actual dewatered-sludge. At the start-up phase (from 0 to the day of maximum methane production  
190 occurred in batch tests), the two semi-continuous digesters were operated the same as 0 or 20 g/kg TS  
191 PFS-added reactors in Section 2.2, respectively. And then, the sludge retention time in the two digesters was  
192 controlled at 20 and 26 d, by withdrawing 50.1 and 38.5 mL of digestion mixtures and replacing with  
193 respective same volume of new sludge each day, respectively, based on the results of the batch experiments in

194 Section 2.2. After 2 months' operation, the daily methane production did not change significantly with time,  
195 and then the measurements of key enzyme activities and microbial community were conducted.

## 196 **2.6. Model-based analysis**

197 Methane production was simulated by the modified Gompertz equation (Eq 1), and kinetic parameters  
198 ( $Mm$ , maximal methane yield potential, mL/g VS or mL/L;  $Rm$ , maximal methane production rate, mL/(g  
199 VS·d) or mL/d or mL/ (L·d);  $\lambda$ , lag-phase time of methane production, d; and  $t$ , digestion time, d;  $e$  is exp(1).)  
200 were calculated using Origin 7.0 software (Lay et al., 1997).

$$201 \quad \text{—————} \quad (1)$$

202 The relationships of PFS concentration with maximal methane yield potential ( $Mm$ , mL/g VSS or mL/L),  
203 maximal methane production rate ( $Rm$ , mL/ (g VS·d) or mL/ (L·d)) and lag phase time of methane production  
204 ( $\lambda$ , d) can be simulated by exponential equations using Origin 7.0 software.

205 The degradation efficiency of model compounds (e.g., BSA, dextran and butyrate) can be calculated by  
206 Eq 2, where  $C_0$  is the initial concentration of model compounds, and  $C_t$  is the concentration of model  
207 compounds measured at a certain fermentation time (d).

$$208 \quad \text{Degradation efficiency (\%)} = 100 \times (C_0 - C_t) / C_0 \quad (2)$$

209 The specific degradation rates of model compounds are obtained by the zero-order kinetic model Eq 3,  
210 where  $X$  is degradation kinetics rate (mg/(L·d)) of model compounds (Batstone et al., 2004).

$$211 \quad C_0 - C_t = X \times t \quad (3)$$

## 212 **2.7. Analytical methods**

213 The measurements of TS, VS, TSS, VSS, COD, soluble carbohydrate, soluble protein, and short-chain  
214 fatty acids were in accordance with the Standard Methods and previous literatures (Rice et al., 2012; Xu et al.,  
215 2019). The COD conversion coefficients of protein and carbohydrate are 1.5 and 1.06, respectively (Li et al.,

216 2020a, 2020b). The volumes of biogas were determined by releasing the pressure in the serum bottle using a  
217 300 mL glass syringe to equilibrate with the room pressure according to the literature (Wang et al., 2019a;  
218 2020). The composition of methane and H<sub>2</sub>S in biogas was analyzed by gas chromatograph equipped with a  
219 thermal conductivity detector according to the method documented in the literatures (Liu et al., 2015; Wang et  
220 al., 2019b). Concentrations of aqueous Fe(III) and Fe(II) were determined using by Inductively Coupled  
221 Plasma Optic Emission Spectrometer (ICAP 6300, Thermo Fisher Scientific, USA), based on the methods  
222 reported previously (Li et al., 2020a). Quantifications of aqueous sulfate and sulfide were performed using  
223 Anion Chromatography System with UV and conductivity detector (ICS-900, Dionex, USA) (Dai et al., 2017;  
224 Gutierrez et al., 2009). The floc size distribution analysis was performed using a Malvern Mastersizer 2000  
225 instrument with a detection range of 0.01 ~ 3500 μm.

226 In addition, the activities of protease, acetate kinase, amidase and coenzyme F420 in semi-continuous  
227 digesters were measured based on the methods reported previously without major modifications (Du et al.,  
228 2020; Fu et al., 2020; Liu et al., 2019). The microbial community in semi-continuous digesters was  
229 determined using high-throughput 16S rRNA gene-based IlluminaMiSeq sequencing, with the 515FmodF  
230 (GTGYCAGCMGCCGCGGTAA) and 806RmodR (GGACTACNVGGGTWTCTAAT) chosen as PCR  
231 primers, and the operational taxonomic units (OTUs) clustered with 97% similarity cutoff (Xu et al., 2020).

## 232 **2.8. Statistical analysis**

233 All experiments were performed in triplicate, and the results were reported as mean ± standard deviation  
234 values. An analysis of variance with least significant difference test was used to assess the significance of  
235 results, and  $p < 0.05$  was considered statistically significant.

## 236 **3. Results and discussion**

### 237 **3.1. Effect of PFS on methane production from anaerobic digestion of WAS**

238 Fig. 1A shows the cumulative methane yield from WAS during anaerobic digestion in the presence of  
239 different levels of PFS. After 32 days of digestion, no significant increment of methane production can be  
240 found in each digester ( $p > 0.05$ , Table S1), indicating that the complete anaerobic digestion had been  
241 achieved. It can be observed that the optimum digestion time for the digester without PFS addition was 20 d,  
242 and at this time the maximal methane yield was obtained (i.e.,  $144.7 \pm 5.0$  mL/g VS). Although similar  
243 tendencies of methane accumulation were also observed in other digesters with PFS addition, the methane  
244 yield was significantly inhibited by PFS. The cumulative methane yield decreased gradually from  $91.7 \pm 0.3\%$   
245 to  $68.0 \pm 0.2\%$  of the control with respect to the increasing PFS levels from 5 to 20 g/kg TS and then further  
246 decreased to  $56.7 \pm 0.2\%$  of the control with increasing PFS level to 40 g/kg TS. Further investigation  
247 determined that the maximal methane yield showed a well negative correlation with the PFS levels in the  
248 sludge ( $Y = 152.14 - 3.15 \times X + 0.04 \times X^2$ ,  $R^2 = 0.9963$ , Fig. S2).

249 To further understand the impact of PFS on anaerobic sludge digestion, the anaerobic digestion kinetics  
250 were estimated using the modified Gompertz model (Eq 2). The simulated methane production curves are  
251 shown in Fig. 1A, which indicates the fit of methane production to the used model was satisfactory ( $R^2 > 0.96$   
252 in all studies cases). Three kinetic parameters, i.e., maximal methane yield potential ( $Mm$ ), maximal  
253 methane production rate ( $Rm$ ), and lag phase time ( $\lambda$ ), were obtained and showed in Fig. 1B and Table S2. In  
254 general,  $Mm$  and  $Rm$  decreased exponentially with the increased PFS levels, while the  $\lambda$  presented a reverse  
255 tendency. It has been reported that  $Rm$  is directly relevant to the methanogenic activity, while  $\lambda$  corresponds  
256 with the start-up of digester, and both of them depend on the acclimation period of microorganisms to a proper  
257 substrate and environmental condition in a batch culture (Batstone et al., 2004; Lay et al., 1997). Thus, it can  
258 be concluded that the presence of PFS resulted in the variations of sludge characters and/or digestion system  
259 conditions (e.g., solubilization rate, soluble organic components, floc size), which would be further uncovered

260 in the following text. The above results suggested that the presence of PFS not only decreased biochemical  
261 methane potential but also inhibited the rate of methane production and prolonged the start-up period.

### 262 **3.2. Details of how PFS affects the process of anaerobic digestion**

263 Anaerobic sludge digestion generally contains solubilization of sludge particulate matters, hydrolysis of  
264 macromolecular organics (e.g., protein, carbohydrate), acidogenesis of micromolecular organics (e.g, amino  
265 acid, glucose), and methanogenesis of acetate and CO<sub>2</sub>/H<sub>2</sub> (Fig. S3; Liu et al., 2020a, 2020b; Luo et al.,  
266 2020a). The above results indicated that the terminal product of anaerobic digestion, methane, was  
267 negatively affected by PFS, but it is still unknown the potential effect of PFS on the four successive  
268 bioprocesses. The following analyses were therefore conducted to uncover these gaps.

269 In this study, the effect of PFS on solubilization process was indicated by comparing the concentration of  
270 soluble protein (carbohydrate) in digestion supernate, VSS reduction and floc size of sludge after digestion of  
271 3 days when the solubilized organics from WAS had not been massively bio-consumed for methane  
272 production (Fig. S3; Luo et al., 2020b; Wang et al., 2018). As shown in Fig. 2A, both soluble protein and  
273 carbohydrate decreased significantly in PFS-added reactors except for the lowest PFS dosage ( $p < 0.05$  in all  
274 studied cases). And with the increment of PFS addition, the soluble protein and carbohydrate concentration  
275 decreased gradually. In the 20 g/kg TS PFS-added reactor, the soluble protein and carbohydrate were  
276 respectively  $534.2 \pm 18.0$  mg COD/L and  $121.7 \pm 5.5$  mg COD/L, which were only approximately 66.6% and  
277 69.5% of that in control, suggesting that the addition of PFS inhibited the solubilization process of sludge.  
278 This can be further confirmed by VSS reduction (Fig. 2B), an index of specific meaning for sludge  
279 solubilization (Wu et al., 2019c; Xu et al., 2019). After 3 days' digestion, the VSS reduction in the control  
280 was  $13.2 \pm 0.5\%$  whereas the corresponding value was only  $7.3 \pm 0.4\%$  in 40 g/kg TS PFS-added reactor.  
281 The higher the PFS dosage, the lower the sludge solubilization, and the less the levels of organic substrates

282 provided for subsequent methane-producing process (Fig. 2D,  $R^2 = 0.9822$ ).

283 The solubilization of sludge is defectively relevant to its floc size (Xu et al., 2020). Fig. 2C illustrates  
284 the effect of PFS on the floc size distribution of sludge after digestion of 3 days. The distribution of floc size  
285 moved to the increasing direction along with the PFS dosage. The medium diameter of raw sludge was  $34.7$   
286  $\pm 2.0 \mu\text{m}$ . With the addition of 20 g PFS/kg TS for instance, the medium diameter raised to  $58.3 \pm 2.8 \mu\text{m}$ ,  
287 indicating the physical enmeshment increased with the increasing addition of PFS dosage. As a result of  
288 physical enmeshment which increased the mass transfer resistance between the organics substrates and  
289 microbes (Chu et al., 2005), it can be revealed why the increase addition of PFS inhibited the sludge  
290 solubilization process, as well as the methane production (Fig. 2D,  $R^2 = 0.9764$ ).

291 The results of batch tests using model organics as substrates were summarized in Table S3 and Fig. S4.  
292 It can be observed that the degradations of all tested substrates were affected, and the higher the PFS dosage  
293 the lower the degradation efficiency. Fig. 3 shows the specific degradation rates of model compounds  
294 obtained by the zero-order kinetic model. It can be seen that the specific degradation rates of BSA, dextran,  
295 L-alanine, glucose, acetate, and hydrogen in the control were 1.39, 0.51, 1.02, 0.24, 0.89, and 0.089 L/(L·d),  
296 respectively. However, in the presence of 20 g/kg TS PFS, these values decreased to 0.69, 0.27, 0.58, 0.13,  
297 0.49 and 0.040 L/(L·d), and which was 49.6%, 52.9%, 56.9%, 54.2%, 55.1%, and 40.8% of that in control,  
298 respectively, suggesting that the process of hydrolysis, acidogenesis, and methanogenesis involved in  
299 anaerobic digestion were severely restrained by PFS. As indicated by the correlation analysis in Fig. S5, the  
300 degradation rate of these model compounds showed a linear correlation with methane production rate in Fig.  
301 1B with  $R^2$  values higher than 0.97. In addition, the activities of key enzymes (i.e., protease, acetate kinase,  
302 and coenzyme F420) in the semi-continuous digesters were detected and the results were out lined in Fig. S6.  
303 It can be found that the relative activities of protease, acetate kinase, and coenzyme F420, which respectively

304 represents the hydrolysis, acidogenesis, and methanogenesis processes in 20 g/kg TS PFS-added digester, was  
305 62.8%, 70.5%, and 57.3% of that in control digester. Thus, it can be speculated that the inhibited enzymes  
306 activity was one reason for the restrained bio-processes (Fig. 3) and the decreased methane production rate  
307 (Fig. 1B). Our previous publications indicated that the polymers such as PAM, an organic macromolecular  
308 flocculant, would cover both organic substrate and anaerobic microbes through its chemical characteristics,  
309 resulting in the deterioration of normal enzyme metabolism (Wang et al., 2018). The hydrolyzed PFS might  
310 play a similar role in the batch digester. Besides the chemical effect, the main derivatives of PFS such as  
311 Fe(III) and sulfate as well as their aggregations, would act as the electron acceptor and cause alterations of  
312 anaerobic biological processes, which were explored in the following analyses.

313 Fig. 4 shows the profile curves of aqueous iron and sulfate (sulfide) in the 20 g/kg TS PFS-added digester.  
314 Dissolved Fe(III) and sulfate decreased gradually along with digestion time, indicating the iron and sulfate  
315 reduction during anaerobic digestion of WAS (Yu et al., 2018). Correspondingly, the Fe(II) increased  
316 substantially from  $0.1 \pm 0.0$  mg/L to  $2.6 \pm 0.1$  mg/L after 4 days of anaerobic digestion, and the sulfide rose  
317 piecemeal in the whole digestion time ( $0.7 \sim 3.5$  mg S/L), indicating the reduction of iron and sulfate which  
318 were driven by iron and sulfate reduction bacteria (IRB and SRB), respectively (Liu et al., 2015). However,  
319 the Fe(II) concentration peaked on day 4 and then decreased immediately to nearly zero on day 16, which  
320 showed an inverse tendency with that of sulfide and could be attributed to the precipitation of Fe(II) with  
321 sulfide. Based on the preliminary balance analysis of iron and sulfur in the anaerobic digestion system, it  
322 can be found that most of them were precipitated and/or adsorbed in sediments ( $> 80\%$ ). Besides the  
323 behavior occurred in liquid phase, there might exist some biological or chemical behaviors of PFS and its  
324 derivatives in sediments that affecting methane-producing process (Van Den Berg et al., 1980; Zeng et al., 2020),  
325 which required to be further investigations in the future.

326 Fig. 4C further illustrates the H<sub>2</sub>S production in control and PFS-added reactors during anaerobic  
327 digestion. In the initial stage of anaerobic digestion (0 ~ 14 days), the H<sub>2</sub>S production in PFS-added reactors  
328 were all lower than that of control. The inhibited production of H<sub>2</sub>S could be attributed to the mass transfer  
329 resistance between the sulfate and sulfate reducing bacteria caused by PFS and the precipitation of sulfide  
330 with Fe(II). However, as anaerobic digestion progressed, the cumulative H<sub>2</sub>S production in PFS-added  
331 reactors exceeded that of control. After 32 days of digestion, the cumulative H<sub>2</sub>S production in the control  
332 was  $93.2 \pm 4.8 \times 10^{-4}$  mL/g VS, and the cumulative production in the 20 and 40 g/kg TS PFS-added reactor  
333 was respectively  $107.3 \pm 5.5 \times 10^{-4}$  and  $118.7 \pm 6.0 \times 10^{-4}$  mL/g VS, which was 115.1% and 127.4% of the  
334 control. In Fig. 4B, the concentration of sulfate in liquid phase showed no significant decrement after  
335 digestion of 14 days, indicating that the occurrence of sulfate reduction in the solid phase and might be  
336 attributed to the reduction of sulfur-containing compounds and the precipitated sulfate substance deserved  
337 from PFS as well. It should be noted that H<sub>2</sub>S might have an inhibitory effect on some methanogenic species,  
338 which might lower the methane production, because the used seed sludge was not sulfate-acclimatised in  
339 present study (Cetecioglu et al., 2019), and this might be another reason for the decreased methane production  
340 in Fig. 1. The above results indicated that the addition of PFS in sludge increased the H<sub>2</sub>S production during  
341 anaerobic digestion, which might damage methanogens in anaerobic digestion system and cause detrimental  
342 problems such as malodors, health hazards and corrosion, need to be taken seriously (Zeng et al., 2020).

### 343 **3.3. Identifying the effect of components of PFS on methane production**

344 Addition of PFS would introduce three components (i.e., hydroxyl polymers, iron, sulfate) into the  
345 digestion system. The different components of PFS might have different effect on sludge anaerobic  
346 digestion, thus their respective impacts on methane yield were identified in this work. Fig. S7 illustrates the  
347 methane production from the components-added reactors along with the digestion time, with the

348 corresponding kinetic parameters of each case shown in Fig. 5A-6C. It was clearly observed that all of these  
349 components from PFS significantly affected the methane production during anaerobic digestion of WAS ( $p <$   
350  $0.05$  in all studied cases).

351 The potassium sulfate, as the substitute of sulfate from PFS, showed a  $17.5 \pm 0.1\%$  inhibition on methane  
352 production. As summarized in Fig. 5D, the sulfate could induce the enrichment of SRB and the competition  
353 of organic substrates with methanogens, as well as the production of hydrogen sulfide in anaerobic digestion  
354 systems (Fig. 4C), which could diffuse across cell membranes and result in protein denaturation and enzyme  
355 inactivation, thereby deteriorate the anaerobic digestion for methane production (Ge et al., 2013; Wei et al.,  
356 2018b; Yuan et al., 2016). This study further confirmed these conclusions. Similarly, the addition of  
357 related dose of ferric sulfate led to a  $11.1 \pm 0.1\%$  decrement of methane production. The reason for this  
358 result might be that the iron content was inadequate for sulfate precipitation.

359 In the presence of ferric chloride, as the substitute of iron from PFS, the methane production of WAS  
360 increased approximately  $17.6 \pm 0.1\%$  compared with that of the control. This result was accorded with the  
361 favorable effect of iron on the anaerobic digestion process previously reported, and as shown in Fig. 5D, the  
362 improvement could be attributed to two aspects: i) being an essential component of microbial cells, and ii)  
363 serving as an accelerator for the hydrolysis-acidification process and biodegradable organic matters generation  
364 (Liu et al., 2015; Wei et al., 2018b; Yu et al., 2015a, 2015b). Compared to PFS, the iron-equivalent ferric  
365 sulfate showed less inhibition ( $11.1\%$  versus  $32.0\%$ ), and this gap might be ascribed to the “hydroxyl  
366 polymers” to some extent. Our previous studies demonstrated that the organic polymer, polyacrylamide,  
367 would induce the aggregation of sludge flocs and increase the mass transfer resistance between the microbes  
368 and organic substrates, thereby deteriorated the anaerobic digestion performances (Wang et al., 2018). It is  
369 worth noting that the hydrolysis of ferric chloride also generates “hydroxide polymers”, however, such species

370 are generally scattered in liquid/solid phase at neutral conditions and easily decomposed by anaerobic  
371 microbes and further utilized for metabolism (Qin et al., 2019; Yu et al., 2015), whereas the PFS-derived  
372 “hydroxide polymers”, could be expressed as  $(Fe_iO_k(OH)_{ij-2k})^{i(3-j)}$  and “multinucleate and multichain-hydroxyl  
373 polymers”, have more nucleus, longer cross-linked chains, punchier aggregation, ~15 times higher  
374 coagulation efficiency ((Jiang et al., 1998; Zouboulis et al., 2008), might play a similar “destroyer” role  
375 toward anaerobic digestion.

376 In addition, based on the variance analysis results within these cases (Fig. 5A-5C), it can be further  
377 demonstrated that among the main components and/or forms of PFS present in anaerobic digester,  
378 “multinucleate and multichain-hydroxyl polymers” and sulfate were unveiled to be the major contributors to  
379 the decreased biomethane potential ( $p < 0.02$ ), and the “multinucleate and multichain-hydroxyl polymers” was  
380 the main buster to the slowed methane-producing rate ( $p < 0.02$ ) and the extended lag time ( $p < 0.01$ ). It  
381 should be noted that the present identification was based on the stoichiometric composition of iron and sulfate  
382 in PFS, with the physical differences between model reagents and the targeted derivatives being ignored. More  
383 works on the detailed biological or chemical behaviors and balance of sulfur and iron in the PFS-added  
384 digestion system, including gas, liquid, and solid phase, should be carried later, although the present results  
385 could provide an insight into the effect of components of PFS on methane production to some degree.

#### 386 **3.4. Effect of PFS on microbial community in long-term operation of semi-continuous digesters**

387 The microbial community was measured through high-throughput 16S rRNA sequencing to compare the  
388 community diversity, structure, and function in semi-continuous digesters. Fig. S8 illustrates the methane  
389 yield of the two semi-continuous digesters, which further confirmed that the presence of PFS inhibited the  
390 anaerobic methane production. It can be found that after 2 months’ operation, the methane yield in the two  
391 digesters did not change significantly with time, indicating a stable state for microbial community

392 measurement. Ecological diversity indices of the bacteria and archaea, the Simpson evenness, Simpson's E and  
393 Shannon's H indices, decreased in the PFS-added reactor (Fig. 6A). In the presence of 20 g/kg TS PFS, the  
394 richness, evenness and diversity metrics of 0.97 OTUs decreased from  $1800 \pm 154$ ,  $5.767 \pm 0.620$  and  $0.063 \pm$   
395  $0.013$  to  $1466 \pm 130$ ,  $0.050 \pm 0.009$  and  $5.214 \pm 0.480$ . The possible reason for this effect might contribute  
396 to the biotoxicity of PFS to anaerobic digestion process. The results can be further revealed by a bipartite  
397 association network showing the associations of bacteria and archaea in each digester at genus level (Fig. 6B  
398 and 7C). It can be found that of these species, 88.7% bacteria and 100% archaea in PFS-added digester were  
399 associated with the control, indicating that the basic similarity of the communities in the two digesters.  
400 However, at PFS-added digester, the exclusive species regardless of bacteria and archaea were significantly  
401 lower than that of the control digester. These results suggest that the presence of PFS can reduce microbial  
402 alpha diversity of digester.

403 Sunburst plot based community analysis was carried out to reveal how the PFS affected the community  
404 structure of bacteria and archaea from the phylum level to genus level (Fig. 7). For the bacteria community  
405 posted in Fig. 7A, the *Chloroflexi*, *Bacteroidetes* and *Proteobacteria*, were the dominant phyla in two detected  
406 digesters regardless of the presence or absence of PFS, and no new dominant species emerged in the  
407 PFS-added digesters, which were consistent with the results outlined in Fig. 6. The predominant genera of  
408 bacteria were *vadinHA17* sp, *Anaerolineaceae\_norank* sp, and *Longilinea* sp, which respectively affiliated to  
409 phyla *Bacteroidetes*, *Chloroflexi*, and *Chloroflexi.*, in the presence of 20 g/kg TS PFS, varied much from that  
410 of the control in relative abundances. The *Anaerolineaceae\_norank* sp and *Longilinea* sp, which were  
411 reported to have ability to degrade some carbohydrates and be associated to syntrophic communities of  
412 bacteria and methanogenic archaea (Xu et al., 2017; Yamada et al., 2007), decreased to 7.7% and 8.8% in 20  
413 g/kg TS PFS-added digester (13.1% and 12.7% in control digester), respectively. Similar trends could be

414 found in genera *Anaerolineaceae\_noclassified* sp, *Leptolinea* sp, and *BDI-7-clade* sp, which have been  
415 documented to be hydrocarbon degraders and main participators in hydrolysis-acidification process (Kim et  
416 al., 2012; Liu et al., 2019), indicating that the PFS caused the shift of the microbial structure toward the  
417 direction against hydrolysis and acidogenesis, which were in agreement with the deteriorated performances in  
418 hydrolysis and acidogenesis model experiments (Fig. 3). The *vadinHA17* sp, which was usually found in the  
419 environment rich in refractory and/or complex organics such as pectin and hemicellulose, accounted for 20.3%  
420 in the 20 g/kg TS PFS-added digester, whereas this value was only 13.2% in the control, was assumed to be  
421 the despondence for the formed multinucleate and multichain-hydroxyl polymers derived from PFS (Liu et al.,  
422 2019; Nelson et al., 2011). Specially, the genera of *thermodesulfovibrio* sp, belonged to phyla *Nitrospirae*,  
423 and is capable of sulfate and or iron reducing, was enriched with the presence of PFS (3.04% versus 1.97%),  
424 reflecting that the PFS stimulated the sulfate and/or iron reducing bacteria during anaerobic digestion  
425 (Sekiguchi et al., 2008).

426 Regarding the archaeal community, the predominant genera of methanogens were *Methanosaeta* sp,  
427 *Methanobacterium* sp, *Candidatus.Methanofastidiosum* sp, and *Methanolinea* sp, which accounted for 47.2%,  
428 21.9%, 11.9%, and 6.65% of archaea 16S rRNA gene sequences of the control (Fig. 7B). In the presence of  
429 PFS (e.g., 20 g/kg TS), the structure of predominant genera of methanogens did not differ much from that of  
430 the control, but their relative abundance shifted largely. The genera of *Methanobacterium* sp,  
431 *Candidatus.Methanofastidiosum* sp and *Methanolinea* sp, which have been proved to be hydrogenotrophic  
432 methanogens (He et al., 2019; Sakai et al., 2012), dropped to 11.5%, 7.83%, and 3.13%, respectively. The  
433 genera of *Methanosaeta* sp, the only known strict acetoclastic methanogen (Narayanan et al., 2009), increased  
434 significantly with the addition of 20 g PFS/kg TS (from 47.2% to 68.4%), and the *Woesearchaeia\_norank* sp,  
435 has the ability to use H<sub>2</sub> to reduce methyl compounds to produce CH<sub>4</sub> (Gründger et al., 2019), also increased

436 to 3.93%. These facts suggested that the pathway of CH<sub>4</sub> production was partially transferred from  
437 hydrogenotrophic to acetotrophic methanogenesis, which further confirmed that the presence of PFS showed a  
438 severer inhibition on hydrogenotrophic methanogens than acetotrophic methanogens, as shown in Fig. 2C.  
439 Previous studies demonstrated that the diffusion of gas in polymer solutions is far less effective than  
440 low-molecular organics, thus it can be speculated that the severe mass transfer resistance of H<sub>2</sub> between the  
441 syntrophs and methanogens caused by the formed multinucleate and multichain-hydroxyl polymers of PFS  
442 were the contributors to the transferred methanogenesis pathway and inhibited hydrogenotrophic methanogens  
443 (Caulfield et al., 2002; Kawashima et al., 1990). In addition, as shown in Fig. 7A, PFS stimulated the sulfate  
444 and/or iron reducing bacteria during anaerobic digestion (i.e., *thermodesulfovibrio* sp). The genera of  
445 *thermodesulfovibrio* sp, was proven to be a generalist participating in the metabolism of anaerobic  
446 intermediates and use pyruvate, and hydrogen as electron donors in the presence of sulfate (Liang et al., 2016).  
447 And more importantly, they have a higher appetency for hydrogen than methanogens in the case of  
448 insufficient/limited hydrogen content, which might be the other reasons for the shift and/or differences  
449 deciphered above (Harada et al., 1994).

### 450 **3.6. Implications for wastewater and sludge treatments**

451 This study investigated the effects of PFS on anaerobic digestion of WAS and underlying mechanisms for  
452 the first time, through batch and long-term tests using either synthetic wastewaters or real WAS as the  
453 digestion substrates. It was found that the presence of PFS resulted in a terrible performance of anaerobic  
454 sludge digestion. From macro to micro levels, it was revealed that the physical enmeshment caused by PFS  
455 significantly lessened the levels of organic substrates for methane-producing process, the presence of PFS  
456 severely restrained the anaerobic bio-processes of hydrolysis, acidogenesis and methanogenesis by lowering  
457 down the activities of the relevant enzymes, and meanwhile, the produced or surplus sulfide from PFS also

458 had a toxicity on methanogens (Fig. 8), which could be confirmed by microbial community results.  
459 Especially, PFS's inhibitions to hydrogenotrophic methanogenesis was much severer than that to acetotrophic  
460 methanogenesis, which could be further supported by the elevated abundances of *Methanosaeta* sp and the  
461 dropped abundances of *Methanobacterium* sp in PFS-added digester, and probably due to the severe mass  
462 transfer resistance of hydrogen between the syntrophs and methanogens caused by PFS, as well as the higher  
463 hydrogen appetency of PFS-induced sulfate reducing bacteria.

464 Considering the negative effects of PFS on anaerobic sludge digestion, more attentions should be paid  
465 when using in wastewater management and sludge treatments systems, to avoid its entrance to the WAS  
466 anaerobic system. Although the use of flocculants such as PFS is inevitable, there are two optimal solutions  
467 to lower down the possibility of PFS entering sludge anaerobic system. One is to compound with other no or  
468 less toxicity flocculants such as ferric chloride, chitosan, starch, and other microbial flocculants, by which the  
469 usage amount of PFS could be significantly reduced in flocculants process (Wei et al., 2018a; Yu et al., 2015).  
470 The other one is to lessen the percentage of sulfate through modifying the PFS using some natural compounds  
471 such as sodium alginate and chitosan (Wu et al., 2019a, 2019b). The sewage and sludge treatment should be  
472 coupled as a whole, one should not consider only the performances enhancement of sewage pretreatment  
473 and/or sludge dewatering by using plenty of flocculants and ignore the flocculant's potential effect to other  
474 biochemical processes, such as biological nitrogen and phosphorus removal, anaerobic digestion. In addition,  
475 the physical enmeshment caused by PFS and high TS of sludge was found to be one of the reasons for the  
476 decreased methane production, thus, it can be speculated that diluting the PFS-contained sludge might be an  
477 effective way for mitigating PFS's negative effects. However, it is noticeable that this work mainly aimed to  
478 provide insights into the PFS-involved anaerobic digestion system, more effects should be devoted to  
479 mitigating PFS's negative effects in the future.

## 480 **4. Conclusion**

481 This study revealed the effects of PFS on anaerobic digestion of WAS and underlying mechanisms for the  
482 first time. The main conclusions are: (1) The presence of PFS not only decreased biochemical methane  
483 potential but also inhibited the methane production rate and prolonged the start-up period during anaerobic  
484 sludge digestion. (2) PFS significantly lessened the levels of organic substrates for methane-producing  
485 process, and meanwhile severely restrained the anaerobic bio-processes of hydrolysis, acidogenesis and  
486 methanogenesis. (3) PFS decreased the microbial diversity and caused the shift of microbial structure  
487 toward the direction against hydrolysis, acidogenesis and methanogenesis. (4) “multinucleate and  
488 multichain-hydroxyl polymers” and sulfate from PFS were unveiled to be the major contributors to the  
489 decreased biomethane potential, and the “multinucleate and multichain-hydroxyl polymers” were the chief  
490 buster to the slowed methane-producing rate and the extended lag time. The findings obtained herein would  
491 make a sound contribution to the mitigation of PFS’s negative effects in wastewater and/or WAS treatment  
492 system in the future.

## 493 **Acknowledgments**

494 This study was financially supported by Huxiang High Level Talent Gathering Project (2019RS1029),  
495 and the project of National Natural Science Foundation of China (52000063). We greatly thank the Shanghai  
496 Tongji Gao Tingyao Environmental Science & Technology Development Foundation for the partial support.

## 497 **Appendix A. Supplementary data**

498 This file contains analytical methods, Table S1 – S3 and Fig. S1 – S8.

## 499 **References**

500 Angelidaki, I., Alves, M. Bolzonella, D. Borzacconi, L. Campos, J. L. Guwy, A. J. Kalyuzhnyi, S.  
501 Jenicek, P. Van Lier, J. B., 2009. Defining the biomethane potential (BMP) of solid organic  
502 wastes and energy crops: a proposed protocol for batch assays. *Water Sci. Technol.* 59, 927-934.

503 Appels, L., Baeyens, J., Degève, J., Dewil, R., 2008. Principles and potential of the anaerobic  
504 digestion of waste-activated sludge. *Prog. Energy Combust. Sci.* 34, 755-781.

505 Bao, H., Jiang, L., Chen, C., Yang, C., He, Z., Feng, Y., Cai, W., Liu, W., Wang, A., 2015.  
506 Combination of ultrasound and Fenton treatment for improving the hydrolysis and acidification  
507 of waste activated sludge. *RSC Adv.* 5, 48468-48473.

508 Batstone, D.J., Torrijos, M., Ruiz, C., Schmidt, J.E., 2004. Use of an anaerobic sequencing batch  
509 reactor for parameter estimation in modelling of anaerobic digestion. *Water Sci. Technol.* 50(10),  
510 295.

511 Bratby, J., 2016. *Coagulation and Flocculation in Water and Wastewater Treatment*, third ed. IWA  
512 Publishing, UK.

513 Caulfield, M., Qiao, G, Solomon, D., 2002. Some Aspects of the Properties and Degradation of  
514 Polyacrylamides. *Chem. Rev.* 102, 3067-3083.

515 Cetecioglu, Z., Dolfing, J., Taylor, J., Purdy, K., Eyice, O., 2019. COD/sulfate ratio does not affect  
516 the methane yield and microbial diversity in anaerobic digesters. *Water Res.* 155, 444-454.

517 Chu, C.P., Tsai, D.G., Lee, D.J., Tay, J.H., 2005. Size-dependent anaerobic digestion rates of  
518 flocculated activated sludge: role of intra- floc mass transfer resistance. *J. Environ. Manag.* 76,  
519 239-244.

520 Chu, Y.-B., Li, M., Liu, J.-W., Xu, W., Cheng, S.-H., Zhao, H.-Z., 2018. Molecular insights into the  
521 mechanism and the efficiency-structure relationship of phosphorus removal by coagulation.  
522 *Water Res.* 147, 195-203.

523 Dai, X., Hu, C., Zhang, D., Chen, Y., 2017. A new method for the simultaneous enhancement of  
524 methane yield and reduction of hydrogen sulfide production in the anaerobic digestion of waste  
525 activated sludge. *Bioresour. Technol.* 243, 914-921.

526 Du, M., Liu, X., Wang, D., Yang, Q., Duan, A., Chen, H., Liu, Y., Wang, Q., Ni, B.-J., 2020.  
527 Understanding the fate and impact of capsaicin in anaerobic co-digestion of food waste and  
528 waste activated sludge. *Water Res.* 116539.

529 Fu, Q., Wang, D., Li, X., Yang, Q., Xu, Q., Ni, B.-J., Wang, Q., Liu, X., 2021. Towards hydrogen  
530 production from waste activated sludge: principles, challenges and perspectives. *Renew. Sust.*  
531 *Energ. Rev.* 135, 110283

532 Ge, H., Zhang, L., Batstone Damien, J., Keller, J., Yuan, Z., 2013. Impact of Iron Salt Dosage to  
533 Sewers on Downstream Anaerobic Sludge Digesters: Sulfide Control and Methane Production. *J*  
534 *Environ Eng.* 139, 594-601.

535 Ghyoot, W., Verstraete, W., 1997. Anaerobic digestion of primary sludge from chemical  
536 pre-precipitation. *Wat. Sci. Tech.* 36, 357-365.

537 Gründger, F., Carrier, V., Svenning, M.M., Panieri, G., Vonnahme, T.R., Klasek, S., Niemann, H.,  
538 2019. Methane-fuelled biofilms predominantly composed of methanotrophic ANME-1 in Arctic  
539 gas hydrate-related sediments. *Sci. Rep.* 9, 9725.

540 Gutierrez, O., Park, D., Sharma, K.R., Yuan, Z., 2009. Effects of long-term pH elevation on the  
541 sulfate-reducing and methanogenic activities of anaerobic sewer biofilms. *Water Res.* 43,  
542 2549-2557.

543 Hansen, K.H., Angelidaki, I., Ahring, B.K., 1999. Improving thermophilic anaerobic digestion of  
544 swine manure. *Water Res.* 33, 1805-1810.

545 Harada, H., Uemura, S., Momonoi, K., 1994. Interaction between sulfate-reducing bacteria and  
546 methane-producing bacteria in UASB reactors fed with low strength wastes containing different  
547 levels of sulfate. *Water Res.* 28, 355-367.

548 He, Z.-W., Liu, W.-Z., Tang, C.-C., Liang, B., Guo, Z.-C., Wang, L., Ren, Y.-X., Wang, A.-J., 2019.  
549 Performance and microbial community responses of anaerobic digestion of waste activated  
550 sludge to residual benzalkonium chlorides. *Energy Convers Manage.* 202, 112211.

551 Jiang, J.Q., Graham, N.J.D., 1998. Observations of the comparative hydrolysis/precipitation  
552 behaviour of polyferric sulphate and ferric sulphate. *Water Res.* 32, 930-935.

553 Kawashima, M., Tanaka, H, Sakaguchi, M., 1990. The characteristics of a gas diffusion hybrid  
554 polymer electrode in the oxygen reduction reaction. *J. Electroanal. Chem.* 286, 123-131.

555 Kim, J.E., Eom, H.-J., Kim, Y., Ahn, J.E., Kim, J.H., Han, N.S., 2012. Enhancing acid tolerance of  
556 *Leuconostoc mesenteroides* with glutathione. *Biotechnol. Lett.* 34, 683-687.

557 Lay, J.-J., Li, Y.-Y., Noike, T., 1997. Influences of pH and moisture content on the methane  
558 production in high-solids sludge digestion. *Water Res.* 31, 1518-1524.

559 Li, Y., Xu, Q., Liu, X., Wang, Y., Wang, D., Yang, G., Yuan, X., Yang, F., Huang, J., Wu, Z. 2020a.  
560 Peroxide/Zero-valent iron (Fe<sup>0</sup>) pretreatment for promoting dewaterability of anaerobically  
561 digested sludge: A mechanistic study. *J. Hazard. Mater.* 400, 123112.

562 Li, Y, Zhu, Y, Wang, D, Yang, G, Pan, L, Wang, Q, Ni, B-J, Li, H, Yuan, X, Jiang, L, Tang, W, 2020b.  
563 Fe(II) catalyzing sodium percarbonate facilitates the dewaterability of waste activated sludge:  
564 Performance, mechanism, and implication. *Water Res.* 174, 115626.

565 Liang, B., Wang, L-Y., Zhou, Z., Mbadinga, S., Zhou, L., Liu, J-F., Yang, S-Z., Gu, J-D., Mu, B-Z.,  
566 2016. High frequency of *thermodesulfobivrio* spp. and anaerolineaceae in association with  
567 *Methanoculleus* spp. in a long-term incubation of n-alkanes-degrading methanogenic enrichment  
568 culture. *Front. Microbiol.* 7, 1431.

569 Lin, L., Li, R-H., Yang, Z-Y., Li, X-Y., 2017. Effect of coagulant on acidogenic fermentation of  
570 sludge from enhanced primary sedimentation for resource recovery: Comparison between FeCl<sub>3</sub>  
571 and PACl. *Chem. Eng. J.* 325, 681-689.

572 Lin, L., Li, X-Y., 2018. Effects of pH adjustment on the hydrolysis of Al-enhanced primary  
573 sedimentation sludge for volatile fatty acid production. *Chem. Eng. J.* 346, 50-56.

574 Liu, X., Du, M., Yang, J., Wu, Y., Xu, Q., Wang, D., Yang, Q., Yang, G., Li, X., 2020a. Sulfite  
575 serving as a pretreatment method for alkaline fermentation to enhance short-chain fatty acid  
576 production from waste activated sludge. *Chem. Eng. J.* 385, 123991.

577 Liu, X., Huang, X., Wu, Y., Xu, Q., Du, M., Wang, D., Yang, Q., Liu, Y., Ni, B-J., Yang, G., Yang, F.,  
578 Wang, Q., 2020b. Activation of nitrite by freezing process for anaerobic digestion enhancement  
579 of waste activated sludge: Performance and mechanisms. *Chem. Eng. J.* 387, 124147.

580 Liu, X., Xu, Q., Wang, D., Wu, Y., Yang, Q., Liu, Y., Wang, Q., Li, X., Li, H., Zeng, G., Yang, G.,  
581 2019. Unveiling the mechanisms of how cationic polyacrylamide affects short-chain fatty acids  
582 accumulation during long-term anaerobic fermentation of waste activated sludge. *Water Res.*  
583 155, 142-151.

584 Liu, Y., Zhang, Y., Ni, B.-J., 2015. Evaluating enhanced sulfate reduction and optimized volatile fatty  
585 acids (VFA) composition in anaerobic reactor by Fe (III) addition. *Environ. Sci. Technol.* 49,  
586 2123-2131.

587 Luo, J., Huang, W., Guo, W., Ge, R., Zhang, Q., Fang, F., Fegn, Q., Cao, J., Wu, Y., 2020a. Novel  
588 strategy to stimulate the food wastes anaerobic fermentation performance by eggshell wastes  
589 conditioning and the underlying mechanisms. *Chem. Eng. J.* 398, 125560.

590 Luo, J., Zhang, Q., Zhao, J., Wu, Y., Wu, L., Li, H., Tang, M., Sun, Y., Guo, W., Feng, Q., Cao, J.,  
591 Wang, D., 2020b. Potential influences of exogenous pollutants occurred in waste activated  
592 sludge on anaerobic digestion: A review. *J. Hazard Mater.* 383, 121176.

593 Moussas, P.A., Zouboulis, A.I., 2009. A new inorganic–organic composite coagulant, consisting of  
594 Polyferric Sulphate (PFS) and Polyacrylamide (PAA). *Water Res.* 43, 3511-3524.

595 Narayanan, N., Krishnakumar, B., Anupama, V.N., Manilal, V.B., 2009. *Methanosaeta* sp., the major  
596 archaeal endosymbiont of *Metopus* es. *Res Microbiol.* 160, 600-607.

597 Nelson, M.C., Morrison, M., Yu, Z., 2011. A meta-analysis of the microbial diversity observed in  
598 anaerobic digesters. *Bioresour. Technol.* 102, 3730-3739.

599 Ozuolmez, D., Na, H., Lever, M.A., Kjeldsen, K.U., Jorgensen, B.B., Plugge, C.M. 2015.  
600 Methanogenic archaea and sulfate reducing bacteria co-cultured on acetate: teamwork or  
601 coexistence? *Front.Microbiol.* 6, 492.

602 Paulo, L.M., Stams, A.J.M., Sousa, D.Z., 2015. Methanogens, sulphate and heavy metals: a complex  
603 system. *Rev. Environ. Sci. Biotechnol.* 14, 537-553.

604 Qiao, W., Takayanagi, K., Li, Q., Shofie, M., Gao, F., Dong, R., Li, Y-Y. 2016. Thermodynamically  
605 enhancing propionic acid degradation by using sulfate as an external electron acceptor in a  
606 thermophilic anaerobic membrane reactor. *Water Res.* 106, 320-329.

607 Qin, Y., Chen, L., Wang, T., Ren, J., Cao, Y., Zhou, S., 2019. Impacts of ferric chloride, ferrous  
608 chloride and solid retention time on the methane-producing and physicochemical  
609 characterization in high-solids sludge anaerobic digestion. *Renew. Energy.* 139, 1290-1298.

610 Rice, E.W., Baird, R.B., Eaton, A.D., Clesceri, L.S., 2012. Standard methods for the examination of  
611 water and wastewater. Washington: APHA, AWWA, WPCR. 1496.

612 Sakai, S., Ehara, M., Tseng, I.C., Yamaguchi, T., Brauer, S.L., Cadillo-Quiroz, H., Zinder, S.H.,  
613 Imachi, H., 2012. *Methanolinea mesophila* sp. nov., a hydrogenotrophic methanogen isolated  
614 from rice field soil, and proposal of the archaeal family *Methanoregulaceae* fam. nov. within the  
615 order *Methanomicrobiales*. *Int J Syst Evol Microbiol.* 62, 1389-1395.

616 Sekiguchi, Y., Muramatsu, M., Imachi, H., Narihiro, T., Ohashi, A., Harada, H., Hanada, S.,  
617 Kamagata, Y., 2008. *Thermodesulfovibrio aggregans* sp. nov. and *Thermodesulfovibrio*  
618 *thiophilus* sp. nov., anaerobic, thermophilic, sulfate-reducing bacteria isolated from thermophilic  
619 methanogenic sludge, and emended description of the genus *Thermodesulfovibrio*. *Int J Syst*  
620 *Evol Microbiol.* 58, 2541-2548.

621 Van Den Berg, L., Lamb, K.A., Murray, W.D., Armstrong, D.W., 1980. Effects of sulphate, iron and  
622 hydrogen on the microbiological conversion of acetic acid to methane. *J. Bacteriol.* 48, 437-447.

623 Wang, D., He, D., Liu, X., Xu, Q., Yang, Q., Li, X., Liu, Y., Wang, Q., Ni, B.-J., Li, H., 2019a. The  
624 underlying mechanism of calcium peroxide pretreatment enhancing methane production from  
625 anaerobic digestion of waste activated sludge. *Water Res.* 164, 114934.

626 Wang, D., Liu, X., Zeng, G., Zhao, J., Liu, Y., Wang, Q., Chen, F., Li, X., Yang, Q., 2018.  
627 Understanding the impact of cationic polyacrylamide on anaerobic digestion of waste activated  
628 sludge. *Water Res.* 130, 281-290.

629 Wang, M., Zhao, Z., Zhang, Y., 2019b. Disposal of Fenton sludge with anaerobic digestion and the  
630 roles of humic acids involved in Fenton sludge. *Water Res.* 163, 114900.

631 Wang, Y., Liu, X., Liu, Y., Wang, D., Xu, Q., Li, X., Yang, Q., Wang, Q., Ni, B-J., Chen, H., 2020.  
632 Enhancement of short-chain fatty acids production from microalgae by potassium ferrate  
633 addition: Feasibility, mechanisms and implications. *Bioresour. Technol.* 318, 124266.

634 Watanabe, Y., Kubo, K., Sato, S., 1999. Application of amphoteric polyelectrolytes for sludge  
635 dewatering. *Langmuir.* 15, 4157-4164.

636 Wei, H., Gao, B., Ren, J., Li, A., Yang, H., 2018a. Coagulation/flocculation in dewatering of sludge:  
637 A review. *Water Res.* 143, 608-631.

638 Wei, J., Hao, X., van Loosdrecht, M.C.M., Li, J., 2018b. Feasibility analysis of anaerobic digestion  
639 of excess sludge enhanced by iron: A review. *Renew Sustain Energy Rev.* 89, 16-26.

640 Wu, J., Zeng, R.J., Zhang, F., Yuan, Z., 2019a. Application of iron-crosslinked sodium alginate for  
641 efficient sulfide control and reduction of oilfield produced water. *Water Res.* 154, 12-20.

642 Wu, J., Zheng, H., Zhang, F., Zeng, R.J., Xing, B., 2019b. Iron-carbon composite from carbonization  
643 of iron-crosslinked sodium alginate for Cr(VI) removal. *Chem. Eng. J.* 362, 21-29.

644 Wu, Y., Liu, X., Wang, D., Chen, Y., Yang, Q., Chen, Y., He, X., Xu, Q., Fu, Q., Du, C., 2020. Iron  
645 electrodes activating persulfate enhances acetic acid production from waste activated sludge. *Chem. Eng. J.* 390, 124580.

647 Xu, D., Liu, S., Chen, Q., Ni, J., 2017. Microbial community compositions in different functional  
648 zones of Carrousel oxidation ditch system for domestic wastewater treatment. *AMB Express.* 7,  
649 40.

650 Xu, Q., Liu, X., Wang, D., Liu, Y., Wang, Q., Ni, B.J., Li, X., Yang, Q., Li, H., 2019. Enhanced  
651 short-chain fatty acids production from waste activated sludge by sophorolipid: Performance,  
652 mechanism, and implication. *Bioresour. Technol.* 262, 456-465.

653 Xu, Q., Huang, Q-S., Wei, W., Sun, J., Dai, X., Ni, B-J., 2020. Improving the treatment of waste  
654 activated sludge using calcium peroxide. *Water Res.* 187, 116440.

655 Xu, R., Li, B., Xiao, E., Y. Young, L., Sun, X., Kong, T., Dong, Y., Wang, Q., Yang, Z., Chen, L., Sun,  
656 W., 2020. Uncovering microbial responses to sharp geochemical gradients in a terrace  
657 contaminated by acid mine drainage. *Environ. Pollut.* 261, 114226.

658 Yamada, T., Imachi, H., Ohashi, A., Harada, H., Hanada, S., Kamagata, Y., Sekiguchi, Y., 2007.  
659 *Bellilinea caldifistulae* gen. nov., sp. nov. and *Longilinea arvoryzae* gen. nov., sp. nov., strictly  
660 anaerobic, filamentous bacteria of the phylum Chloroflexi isolated from methanogenic  
661 propionate-degrading consortia. *Int J Syst Evol Microbiol.* 57, 2299-2306.

662 Yu, B., Lou, Z., Zhang, D., Shan, A., Yuan, H., Zhu, N., Zhang, K., 2015a. Variations of organic  
663 matters and microbial community in thermophilic anaerobic digestion of waste activated sludge  
664 with the addition of ferric salts. *Bioresour. Technol.* 179, 291-298.

665 Yu, B., Shan, A., Zhang, D., Lou, Z., Yuan, H., Huang, X., Zhu, N., Hu, X., 2015b. Dosing time of  
666 ferric chloride to disinhibit the excessive volatile fatty acids in sludge thermophilic anaerobic  
667 digestion system. *Bioresour. Technol.* 189, 154-161.

668 Yu, Q., Jin, X., Zhang, Y., 2018. Sequential pretreatment for cell disintegration of municipal sludge  
669 in a neutral Bio-electro-Fenton system. *Water Res.* 135, 44-56.

670 Yuan, H., Zhu, N., 2016. Progress in inhibition mechanisms and process control of intermediates and  
671 by-products in sewage sludge anaerobic digestion. *Renew Sustain Energy Rev.* 58, 429-438.

672 Zeng, Q., Hao, T., Yuan, Z., Chen, G., 2020. Dewaterability enhancement and sulfide mitigation of  
673 CEPT sludge by electrochemical pretreatment. *Water Res.* 176, 115727.

674 Zhang, J., Yang, H., Li, W., Wen, Y., Fu, X., Chang, J., 2018. Variations of sludge characteristics  
675 during the advanced anaerobic digestion process and the dewaterability of the treated sludge  
676 conditioning with PFS, PDMDAAC and synthesized PFS-PDMDAAC. *Water Sci Technol.* 78,  
677 1189-1198.

678 Zhang, Y., Yang, Z., Xiang, Y., Xu, R., Zheng, Y., Lu, Y., Jia, M., Sun, S., Cao, J., Xiong, W., 2020.  
679 Evolutions of antibiotic resistance genes (ARGs), class 1 integron-integrase (intI1) and potential  
680 hosts of ARGs during sludge anaerobic digestion with the iron nanoparticles addition. *Sci Total*  
681 *Environ.* 724, 138248.

682 Zhen, G., Lu, X., Kato, H., Zhao, Y., Li, Y.-Y., 2017. Overview of pretreatment strategies for  
683 enhancing sewage sludge disintegration and subsequent anaerobic digestion: current advances,  
684 full-scale application and future perspectives. *Renew Sustain Energy Rev.* 69, 559-577.

685 Zhou, G-J., Lin, L., Li, X-Y., Leung, K., 2020. Removal of emerging contaminants from wastewater  
686 during chemically enhanced primary sedimentation and acidogenic sludge fermentation. *Water*  
687 *Res.* 175, 115646.

688 Zouboulis, A.I., Moussas, P.A., Vasilakou, F., 2008. Polyferric sulphate: Preparation, characterisation  
689 and application in coagulation experiments. *J. Hazard. Mat.* 155, 459-468.

690

691 **List of Figures**

692 **Fig. 1.** Cumulative methane production during WAS anaerobic digestion in the presence of different levels  
693 of PFS (A), and correlation between PFS addition and the maximal methane yield potential, maximal methane  
694 production rate and lag phase time from model fit (B). Symbols represent experimental measurements and  
695 curves represent model fit. Error bars represent standard deviations of triplicate tests.

696 **Fig. 2.** Effect of PFS dosage on soluble protein and carbohydrate concentrations (A), VSS reduction (B) and  
697 floc size distribution (C) after digestion of 3 days, as well as the correlation of maximal methane potential  
698 with VSS reduction and floc medium diameter after digestion of 3 days (D). \* represent  $p < 0.05$ , \*\*  
699 represent  $p < 0.02$ , \*\*\* represent  $p < 0.01$ , error bars represent standard deviations of triplicate tests.

700 **Fig. 3.** Effect of PFS on the specific degradation rates of model compounds in batch tests: (A) hydrolysis  
701 process, (B) acidogenesis process, (C) methanogenesis process. The specific degradation rates are modeled  
702 and calculated by Eq 3. The data illustrate in column means the inhibition ratio. Error bars represent  
703 standard deviations of triplicate tests.

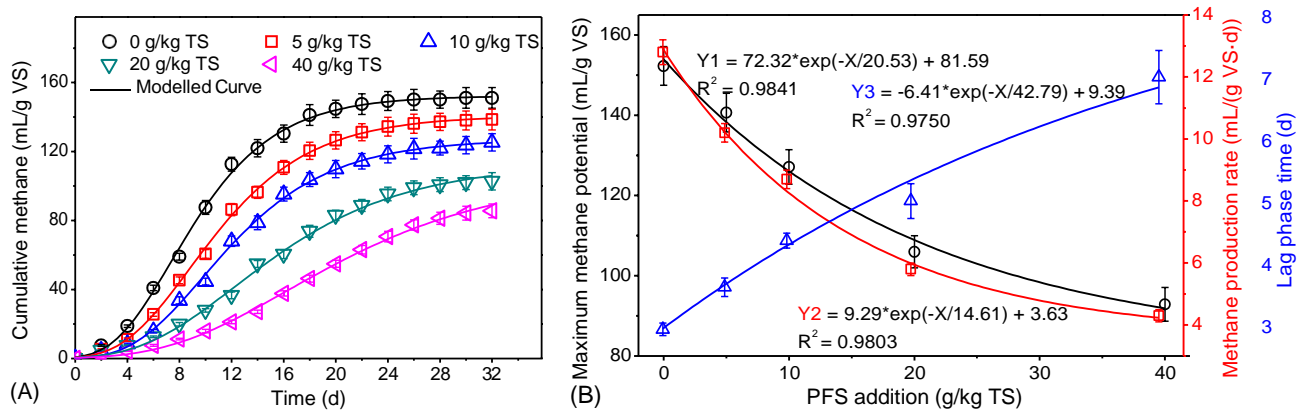
704 **Fig. 4.** Variation of aqueous Fe(III) and Fe(II) in the 20 g/kg TS PFS-added digester during the anaerobic  
705 digestion (A), as well as the concentration of sulfate and sulfide (B). And the effect of PFS on H<sub>2</sub>S  
706 production of anaerobic sludge digestion (C). RO means recalcitrant organics, and BO means biodegradable  
707 organics. Error bars represent standard deviations of triplicate tests.

708 **Fig. 5.** The effect of PFS and its decomposition products on the maximal methane yield potential (A),  
709 maximal methane production rate (B), and lag phase time (C) (compared to that of control), and the potential  
710 effects of components derived from PFS on anaerobic sludge digestion (D). PFS: 20 g/kg TS, ferric sulfate:  
711 14.3 g/kg TS, ferric chloride: 11.6 g/kg TS, potassium sulfate: 20.6 g/kg TS. \* represent  $p < 0.05$ , \*\*  
712 represent  $p < 0.01$ , error bars represent standard deviations of triplicate tests.

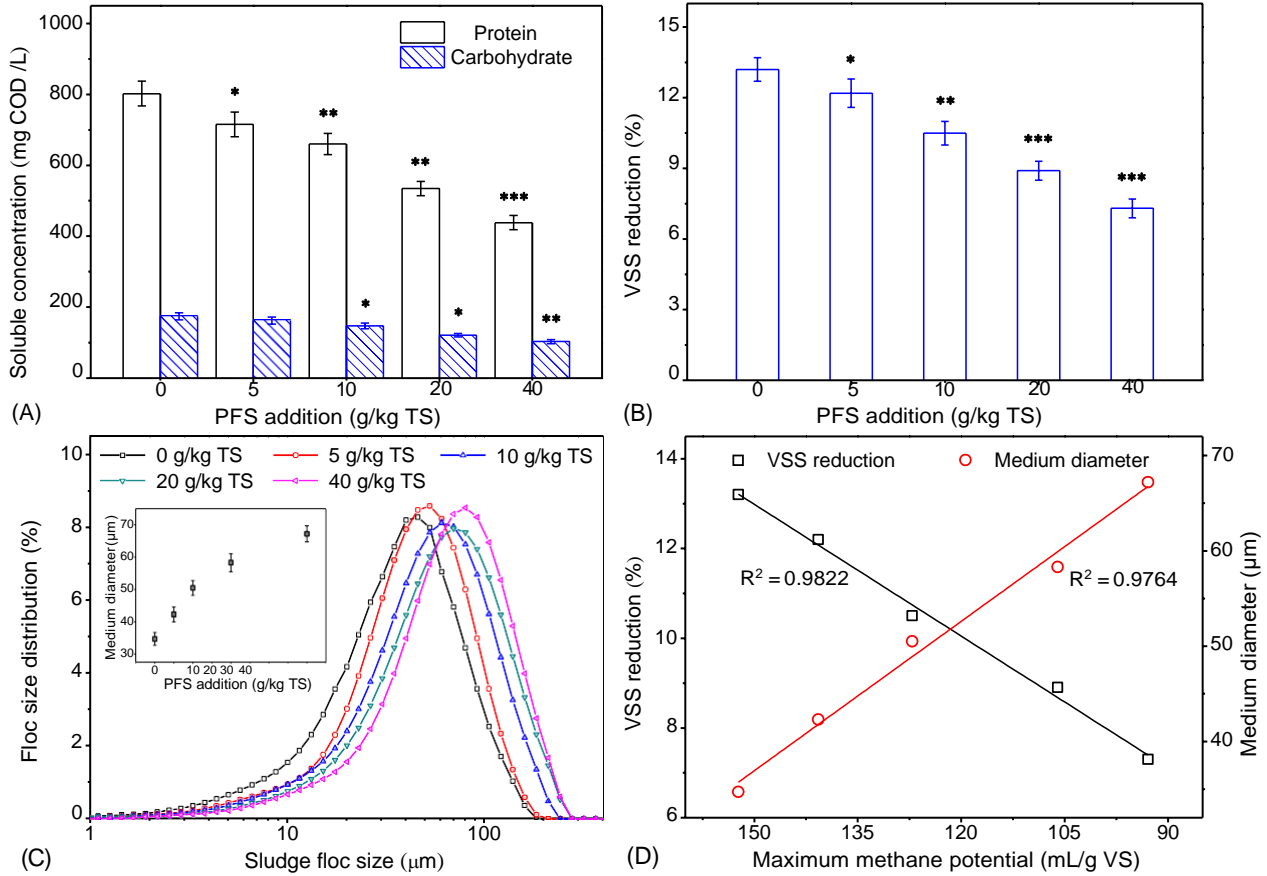
713 **Fig. 6.** Microbial  $\alpha$ -Diversity metrics at different digesters (A), and bipartite association network showing the  
714 associations of bacteria (B) and archaea (C) in each digester at genus level. Node sizes represent relative  
715 abundance (square root) of the species (Genus) in the data sets. Edges represent the association patterns of  
716 individual species with the digesters. The edge-weighted spring-embedded algorithm pulled together species  
717 with similar associations and systems with similar structure.

718 **Fig. 7.** Community analysis sunburst plot of predominant bacteria (A) and archaea (B) on genus level in the  
719 two long-term fermentation digesters. The analysis was based on the species with relative abundance higher  
720 than 0.01. The taxonomies are listed on the right side of each cladogram.

721 **Fig. 8.** Proposed underlying mechanism of PFS's effects on anaerobic sludge digestion.



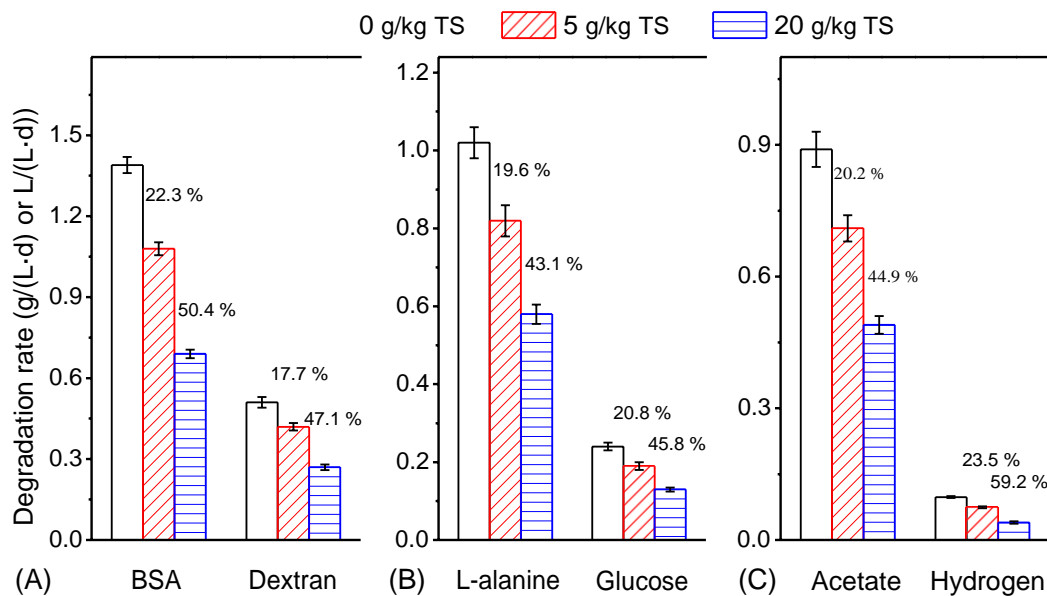
1 (A) Cumulative methane production during WAS anaerobic digestion in the presence of  
2 different levels of PFS (A), and correlation between PFS addition and the maximal methane yield  
3 potential, maximal methane production rate and lag phase time from model fit (B). Symbols  
4 represent experimental measurements and curves represent model fit. Error bars represent standard  
5 deviations of triplicate tests.  
6  
7



8

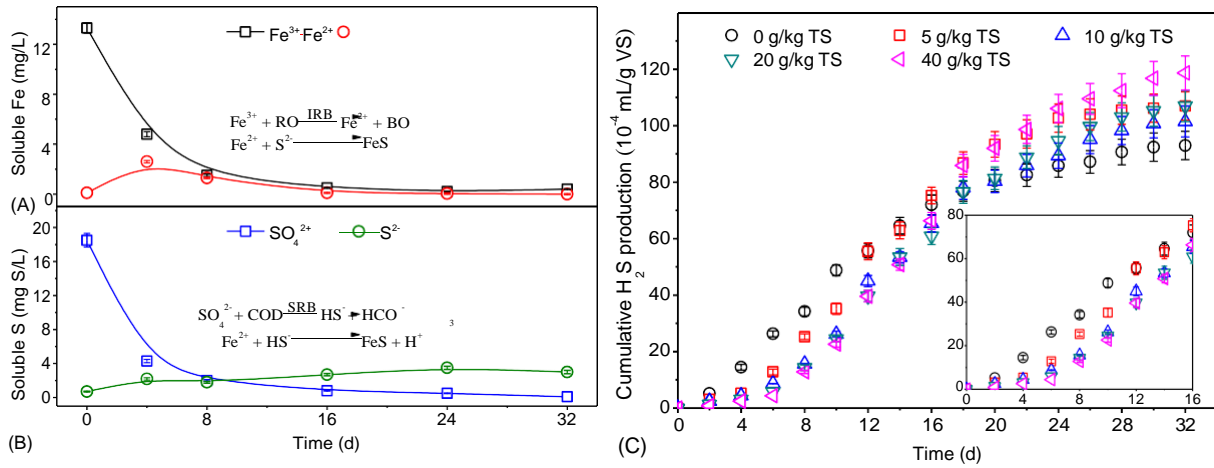
9 **Fig. 2.** Effect of PFS dosage on soluble protein and carbohydrate concentrations (A), VSS  
 10 reduction (B) and floc size distribution (C) after digestion of 3 days, as well as the correlation of  
 11 maximal methane potential with VSS reduction and floc medium diameter after digestion of 3 days  
 12 (D). \* represent  $p < 0.05$ , \*\* represent  $p < 0.02$ , \*\*\* represent  $p < 0.01$ , error bars represent  
 13 standard deviations of triplicate tests.

14



15  
 16 **Fig. 3.** Effect of PFS on the specific degradation rates of model compounds in batch tests: (A)  
 17 hydrolysis process, (B) acidogenesis process, (C) methanogenesis process. The specific  
 18 degradation rates are modeled and calculated by Eq 3. The data illustrate in column means the  
 19 inhibition ratio. Error bars represent standard deviations of triplicate tests.

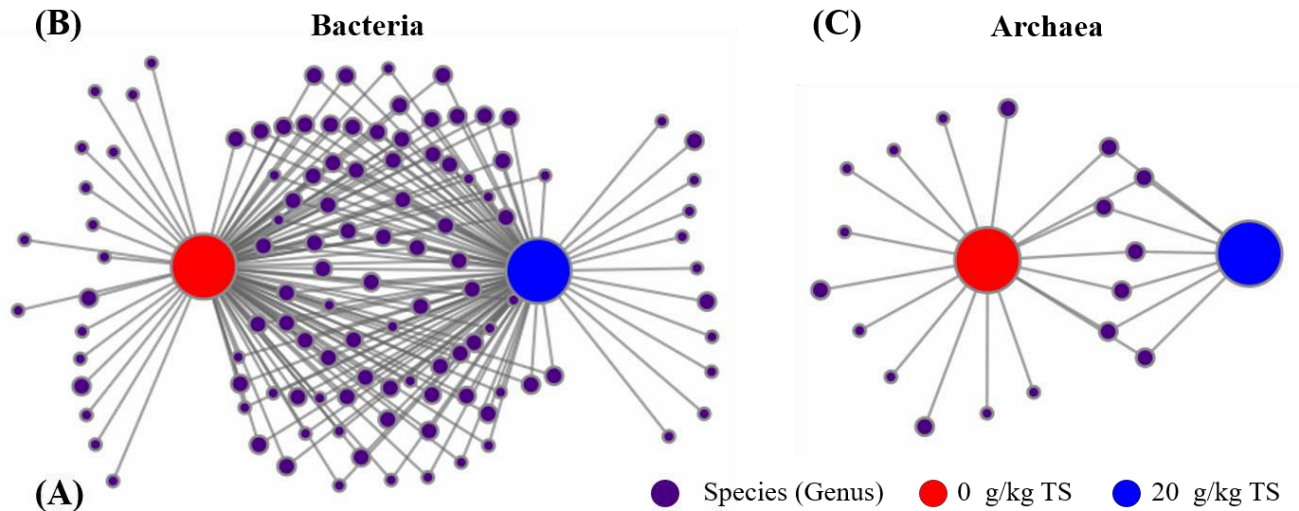
20



21  
22  
23  
24  
25  
26

**Fig. 4.** Variation of aqueous Fe(III) and Fe(II) in the 20 g/kg TS PFS-added digester during the anaerobic digestion (A), as well as the concentration of sulfate and sulfide (B). And the effect of PFS on H<sub>2</sub>S production of anaerobic sludge digestion (C). RO means recalcitrant organics, and BO means biodegradable organics. Error bars represent standard deviations of triplicate tests.





Digester (g/kg TS)	Richness (observed sp.)	Evenness (Simpson's E)	Diversity (Shannon's H)
0	1800 ± 154	0.063 ± 0.013	5.767 ± 0.620
20	1466 ± 130	0.050 ± 0.009	5.214 ± 0.480

34

35

36

37

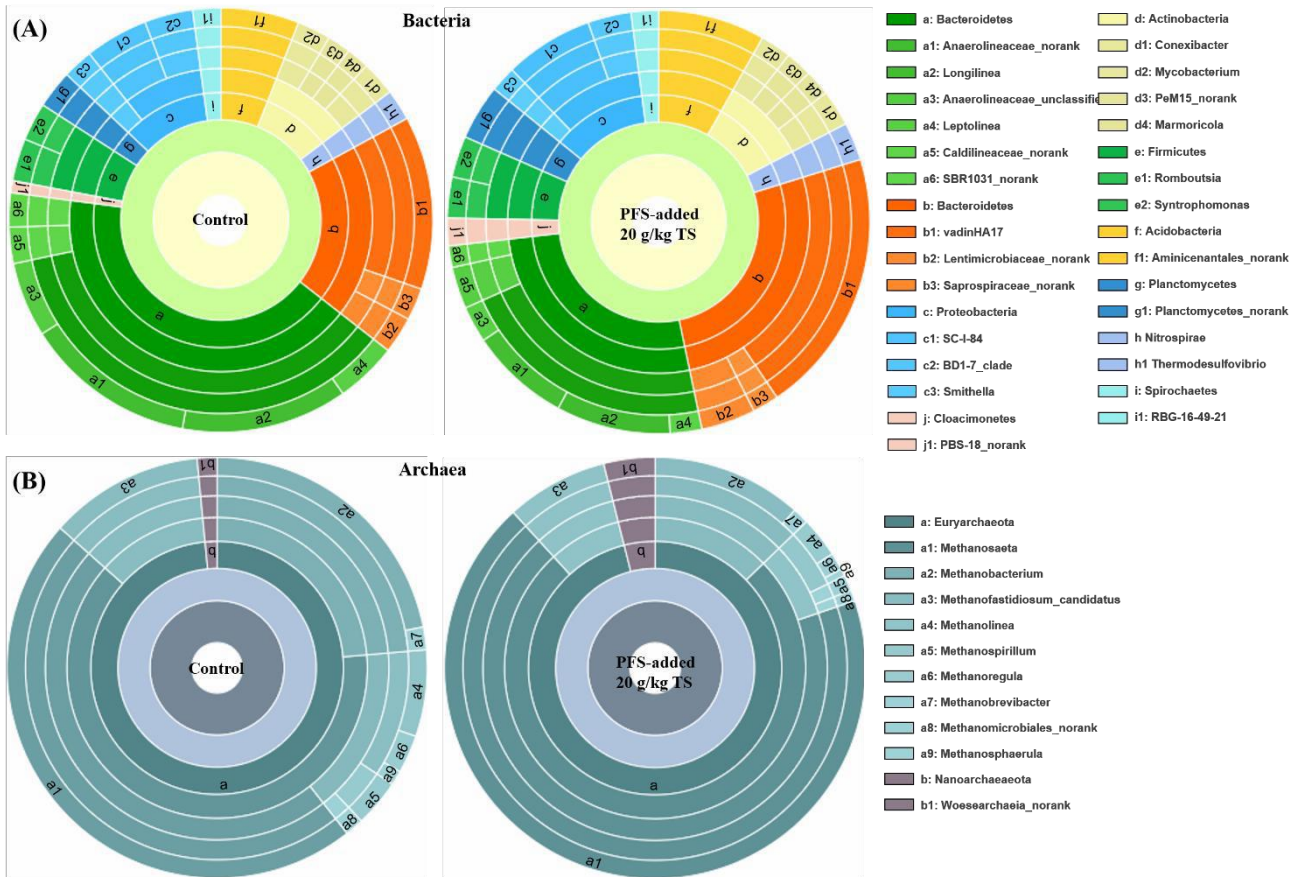
38

39

40

41

**Fig. 6.** Microbial  $\alpha$ -Diversity metrics at different digesters (A), and bipartite association network showing the associations of bacteria (B) and archaea (C) in each digester at genus level. Node sizes represent relative abundance (square root) of the species (Genus) in the data sets. Edges represent the association patterns of individual species with the digesters. The edge-weighted spring-embedded algorithm pulled together species with similar associations and systems with similar structure.



42

43 **Fig. 7.** Community analysis sunburst plot of predominant bacteria (A) and archaea (B) on genus  
 44 level in the two long-term fermentation digesters. The analysis was based on the species with  
 45 relative abundance higher than 0.01. The taxonomies are listed on the right side of each cladogram.

46

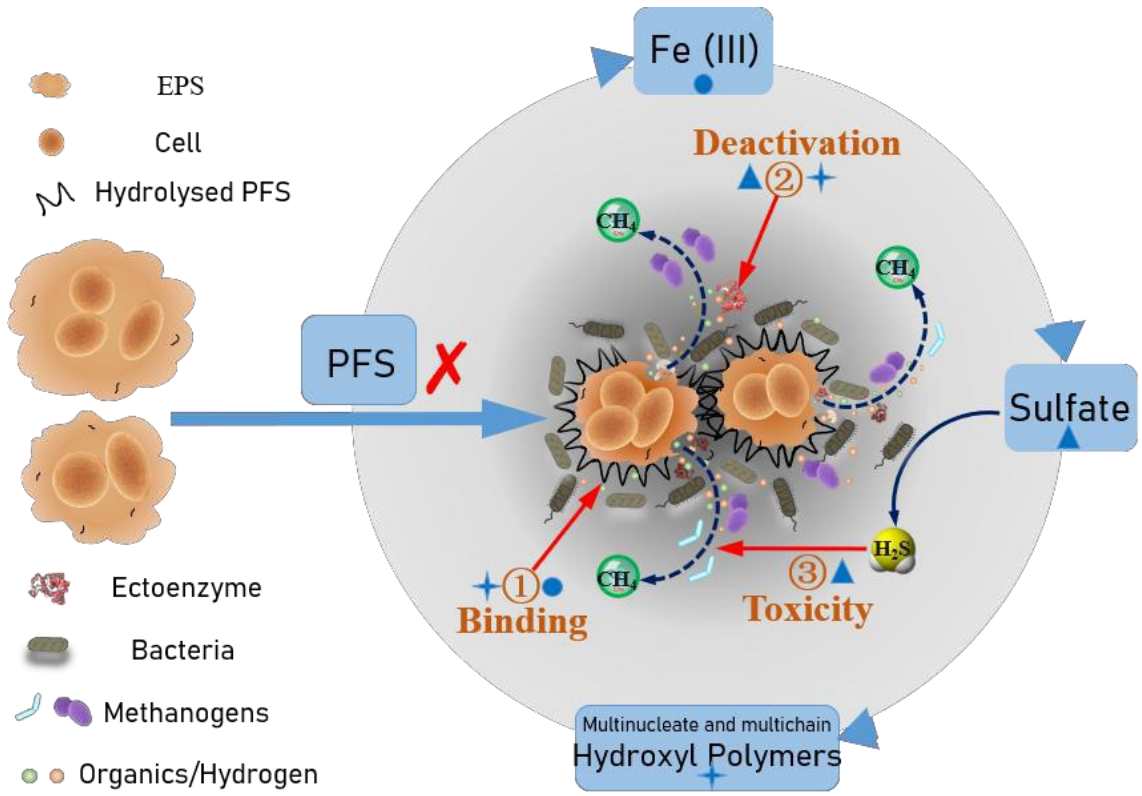


**Fig. 8.** Proposed underlying mechanism of PFS's effects on anaerobic sludge digestion.